# STRESS INTENSITY DISTRIBUTIONS IN NOZZLE CORNER CRACKS OF COMPLEX GEOMETRY

C. W. SMITH, W. H. PETERS *, W. T. HARDRATH, T. S. FLEISCHMAN **

*Department of Engineering Science and Mechanics,*
*Virginia Polytechnic Institute and State University, Blacksburg, Virginia 24061, U.S.A.*

** Currently on leave Institut für Festkörpermechanik, Freiburg, Germany*
*** Currently Research Engineer Central Research Laboratories,*
*Firestone Corp., Akron, Ohio, U.S.A.*

SUMMARY

Cracks at the inner fillet of the juncture between the primary pressure boundary of reactor vessels and inlet or exit nozzles have been a persistant problem for a number of years. Recently, such cracks were observed in boiling water reactors (BWRs) in radial planes at various locations around nozzles. These cracks were believed to have been initiated thermally and thought to be subject to growth due to pressure fluctuations. It was of interest to determine the SIF levels and growth patterns of such cracks in order to determine the most critical cases for use in design.

The complex geometry of such problems render them intractable to closed form analytical solutions, and, as will be shown, are difficult to model numerically due to lack of knowledge of the true crack shape. Over the past decade, the first author and his colleagues have evolved a modelling technique based upon the "frozen stress" method which, under the proper conditions, will simultaneously generate accurate estimates of both flaw shapes and stress intensity factor (SIF) distributions in highly complex three dimensional problems.

In this paper, the technique is applied to scale models of BWRs containing nozzle corner cracks of various depths oriented in a plane: i) normal to the vessel hoop stress direction, ii) parallel to the vessel hoop stress direction, iii) 45° to the vessel hoop stress direction.

Results clearly show that:

1) All flaw growth is non-self-similar with flaw shapes which are not simple quarter circles or quarter ellipses as assumed in numerical analyses.

2) Mechanically grown cracks extend in principal planes of stress. However, for case (ii) the crack may extend in its plane but if only slightly deflected will turn through 90° becoming parallel to (i) (since both planes are principal planes).

3) SIF levels for case (i) are about three times those in (ii) and represent the most severe case for a given flaw depth for design.

4) Case (iii) flaws extend in the plane normal to the nozzle hoop stress direction along the nozzle wall but grow along the plane perpendicular to the hoop vessel stress along the vessel wall. This produces a non-planar flaw. However, SIF levels are significantly lower than for Case I.

5) Collectively, the results indicate that current analyses are conservative for shallow flaws, but may be non-conservative for deep flaws.

Results of the present study suggest that substantial improvement in numerical modelling will result from inserting actual flaw shapes into the models.

## 1. Introduction

Recent advances in the development of high speed digital computers have opened the way for analysts to develop and refine a number of numerical methods (i.e. finite element, boundary integral, influence function, finite difference, alternating and hybrid methods) for estimating stress intensity factor (SIF) distributions in finite three dimensional (3D) cracked body problems such as the nozzle corner crack. Although significant improvements in convergence have resulted, computer code verification in the form of experimental results is still necessary in order to insure that assumptions and restrictions factored into the problem formulation are, indeed, not contrary to the real behavior.

Based upon an idea of G. R. Irwin [1] the first author and his associates have evolved an experimental modelling technique based upon a marriage between the local field equations of linear elastic fracture mechanics and the "frozen stress" method of photoelasticity for measuring SIF distributions along the flaw borders of finite 3D cracked body problems. The analytical foundations of the method as currently applied to Mode I problems are described in [2], and will be omitted here in favor of a description of the experiments and results. However, it should be noted that recent results [3] suggest that the method can also be used to generate flaw shapes corresponding to those observed in fatigue crack growth in steel nozzles when the shape is not known a priori. This paper describes the use of the above method to study flaw geometry and corresponding SIF distributions for nozzle corner cracks in thin walled pressure vessels (Boiling Water Reactors).

## 2. The Problem and Method of Analysis

The dimensions of the scale model of the nozzle studied are given in Figure 1a. A photo of an assembled model is pictured in Figure 1b. Each model contained two diametrically opposite nozzles. The location and orientation of the starter flaws is given in Figure 1c. These starter flaws in radial planes are believed due to thermal shock in the vessel, but their growth is produced by cyclic fluctuations in the internal pressure on the inner pressure boundary. Figure 1d is used to present the notation employed to describe the problem.

Starter cracks were produced in each photoelastic model by striking a sharp blade held normal to the inner fillet at the desired location (Figure 1c). Flaw orientation was initially the same for both nozzles of each vessel. Model sections were then glued together, placed in a stress freezing oven and heated to critical temperature at which the material modulus was about one six-hundredth of the room temperature value and it's optical sensitivity to load about twenty-five times the room temperature value. After a thermal soak to equalize the temperature throughout the model, an internal pressure is applied to extend the flaw and when the flaw is observed to reach it's desired size, the pressure is reduced, terminating flaw growth, and the model is cooled to room temperature under the reduced pressure. Photoelastic stress fringes and deformations produced above critical temperature are retained in the model after unloading due to the relative insensitivity of the material to load at room temperature. Models may then be sliced without altering the fringe and deformation patterns produced above critical temperature. Consequently thin slices are removed at points along the flaw border parallel to the nz plane (Figure 1d) and analyzed photoelastically for the maximum in plane shearing stress. By matching this stress with that provided by the local field equations of linear elastic fracture mechanics corrected for effects of the nonsingular stresses, SIF estimates can be extracted from the photoelastic data [2].

3. Results

Pertinent dimensions and loads for all models tested are given in Table I. Flaw shapes and corresponding SIF distributions for the 0°, 90° and 45° flaw locations are given in Figures 2, 3 and 4 respectively.

The 0° flaws were in a principal plane of the vessel and remained there throughout their growth which is seen to be strongly non-self-similar. Quarter ellipses of the same $a_V$ and $a_N$ values are also drawn to emphasize the "flattening" which occurs near the center of the flaw beginning near $a/T \simeq 0.33$. The SIF distribution curve is seen to reverse its shape as flaw depth and flattening increase. Initial flaws slightly misoriented to the 0° direction will grow back into that plane but will not then have the same shape as if they had started in the 0° plane. Only one slice was obtained from the smallest 0° flaw, and so only one point appears in Fig. 2b for $a/T = 0.087$.

The 90° flaws were also in a principal plane of the vessel, and while they also exhibited non-self-similar growth, both flattening and reversal of curvature of the SIF distributions were absent. In fact, these flaws tended to "bulge" beyond a quarter elliptic shape in the central region. Moreover, if an initial flaw was slightly misoriented, it would not return to the 90° plane but turned towards the 0° orientation instead.

The flaws initially oriented in the 45° plane exhibited a complex growth pattern as seen in Figure 4 which produced non-planar flaws. For small a/T, growth proceeded as two cracks joined at P, a point of discontinuity in the crack front. However, as the flaw grew deeper, the two fronts merged and wiped out the discontinuity, leaving a smooth non-planar flaw surface. This adjustment was accompanied by a reversal in the SIF distribution (Figure 4). In one test, a 45° flaw was driven through the vessel wall and $\gamma$ reached 45° as the flaw found the plane of the vessel hoop stress after it left the field of the nozzle.

4. Comparisons and Conclusions

Most of the analytical work to date on this problem such as [4]-[9] has focused upon 0° flaws because they are expected to be most critically oriented and this study confirms that expectation. In fact, Figure 5 suggests that the SIF level in the 0° flaws will be about three times the level for the 90° flaws for equal internal pressures and flaw sizes. Two of the above noted analyses [6], [9] have been applied in the reactor vessel industry in the U.S.A. Both analyses are numerical and formulate the problem as a quarter-circular flaw undergoing self-similar crack growth and obtain a single "average" value for the Mode I SIF. Figure 6 shows that these models yield conservative predictions for shallow flaws but under predict results for $a/T > 0.5$. Reference [9] also provides predictions for 90° flaws and is compared with results of the present experiments in Figure 7 where it is again seen to be conservative for flaws with $a/T < 0.5$. Reference [9] also can be used to compare with results for the 45° flaws and this is done in Figure 8. However, it must be noted that the flaw geometries here are so different that the comparison is of little value. The sharp drop in the SIF with increasing a/T around $a/T \simeq 0.4$, is accompanied by elimination of the discontinuity at P (Figure 4a).

Conclusions

The results of the present study clearly show that:

i) Flaw growth in nozzle corner cracks is significantly non-self-similar.

ii) When starter cracks enter complex stress fields, the flaw will reorient itself as it grows towards the principal plane of tension even if a non-planar flaw surface results.

iii) Changes in flaw shape due to non-self-similar flaw growth produce significant changes in SIF distributions.

The validity of these conclusions depends upon the extent to which the experimental method employed simulates field conditions. The method has its own limitations; it's use is confined to the elastic behavior of an incompressible material. However, limited studies by the authors suggest that, for Mode I studies, an accuracy of $\pm$ 5% in both SIF values and flaw geometries can be expected provided field conditions involve stable flaw growth under tension-tension loading at stress ratios near unity with only small scale yielding involved. Studies directed towards further delineation of requisite field conditions for simulation by the frozen stress method are continuing.

ACKNOWLEDGEMENTS

The authors gratefully acknowledge the support of the Solid Mechanics Program of the National Science Foundation under Grant No. Eng. 76-20824 for the development of the method used here, the counsel of G. D. Whitman, R. H. Bryan and J. G. Merkle, and the support of the Oak Ridge National Laboratory (Union Carbide Corp.) under subcontract 7015 under W-7405-Eng. 26.

REFERENCES

[1] Irwin, G. R., Discussion, Proceedings of the Society for Experimental Stress Analysis, Vol. 16, No. 1, pp. 92-96, 1958.

[2] Smith, C. W., "Stress Intensity Estimates by a Computer Assisted Photoelastic Method", Fracture Mechanics and Technology, Vol. 1, Sijthoff & Noordhoff, pp. 591-605, March 1977.

[3] Smith, C. W. and Peters, W. H., "Prediction of Flaw Shapes and Stress Intensity Distributions in 3D Problems by the Frozen Stress Method", Preprints of Sixth International Conference on Experimental Stress Analysis, pp. 861-864, September 1978.

[4] Hellen, T. K. and Dowling, A. R., "Three Dimensional Crack Analysis Applied to LWR Nozzle-Cylinder Intersection", International Journal of Pressure Vessels and Piping, Vol. 3, pp. 57-74, 1975.

[5] Reynen, J., "On the Use of Finite Elements in the Fracture Analysis of Pressure Vessel Components", ASME Paper No. 75-PVP-20, June 1975.

[6] Rashid, Y. R. and Gilman, J. D., "Three Dimensional Analysis of Reactor Pressure Vessel Nozzles", Proceedings of the First International Conference on Structural Mechanics in Reactor Technology, Vol. 4, Reactor Pressure Vessels, Part G, Steel Pressure Vessels, pp. 193-213, September 1971.

[7] Schmitt, W., Bartholome, G. Gröstad and Miksch, M., "Calculation of Stress Intensity Factors for Cracks in Nozzles", International Journal of Fracture, Vol. 12, No. 3, pp. 381-390, June 1976.

[8] Broekhoven, M. J. G., "Fatigue and Fracture Behavior of Cracks at Nozzle Corners; Comparison of Theoretical Predictions with Experimental Data", Proceedings of the Third International Conference on Pressure Vessel Technology, Part II, Materials and Fabrication, pp. 839-852, April 1977.

[9] Besuner, P. M., Cohen, L. M. and McLean, J. L., "The Effects of Location, Thermal Stress and Residual Stress on Corner Cracks on Nozzles with Cladding", Transactions of the Fourth International Conference on Structural Mechanics in Reactor Technology, Vol. G, Structural Analysis of Steel Reactor Pressure Vessels, Paper No. G4/5, August 1977.

Table I

Model Dimensions & Loads

| Test No. | Flaw Orientation | p(KPa) | $a_v$(mm) | $a_n$(mm) | a(mm) | a/T |
|---|---|---|---|---|---|---|
| 0[b] | 0° | 4.72 | 1.78 | 3.30 | 1.30 | 0.087 |
| I-Av.[a] | 0° | 3.20 ± 0.16 | 2.62 ± 0.13 | 4.06 ± 0 | 2.08 ± 0 | 0.14 ± 0 |
| IV-B | 0° | 3.11 | 5.09 | 6.37 | 4.32 | 0.29 |
| VI[b] | 0° | 4.72 | 6.35 | 7.11 | 5.02 | 0.33 |
| V-A | 0° | 3.36 | 8.13 | 8.89 | 6.74 | 0.44 |
| II-B | 0° | 2.76 | 10.16 | 10.16 | 7.96 | 0.53 |
| II-A | 0° | 2.76 | 10.67 | 10.67 | 8.56 | 0.57 |
| III-A | 0° | 2.62 | 16.51 | 13.72 | 12.19 | 0.81 |

[a]Avg. of IA, IB, VB

[b]One crack broke through and required resealing
IIIB - Crack was non-planar
IVA - Material inhomogeneity near crack tip

| | | | | | | |
|---|---|---|---|---|---|---|
| IX-B | 90° | 8.52 | 4.35 | 3.13 | 2.67 | 0.176 |
| VII-B | 90° | 13.70 | 3.86 | 3.51 | 3.68 | 0.244 |
| X-B | 90° | 10.30 | 6.30 | 4.70 | 4.30 | 0.287 |
| XI-B | 90° | 12.90 | 6.50 | 4.80 | 4.50 | 0.301 |
| VIII-Av.[c] | 90° | 12.80 ± .10 | 11.60 ± 0.60 | 7.40 ± 0.60 | 8.60 ± 0.30 | 0.57 ± .02 |

[c]Avg. of VIII-A and XI-A
VII-A, VIII-B Defective material near crack
IX-A, X-A Crack turned out of plane

| | | | | | | |
|---|---|---|---|---|---|---|
| XIV-A | 45° | 3.88 | 2.67 | 4.37 | 2.13 | 0.154 |
| XIII-B | 45° | 5.84 | 5.23 | 4.24 | 3.33 | 0.240 |
| XIII-A | 45° | 5.84 | 5.56 | 5.00 | 4.09 | 0.291 |
| XII-B | 45° | 3.86 | 6.60 | 6.25 | 6.02 | 0.458 |
| XIV-B | 45° | 3.88 | 16.26 | 11.18 | 11.94 | 0.777 |

XII-A - Crack broke through surface

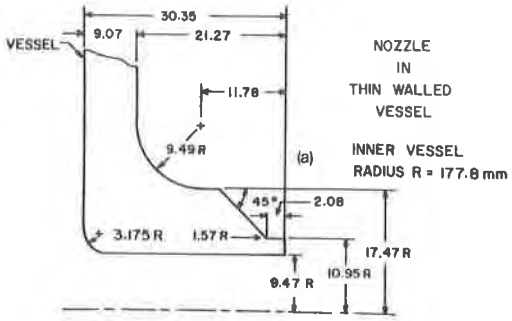



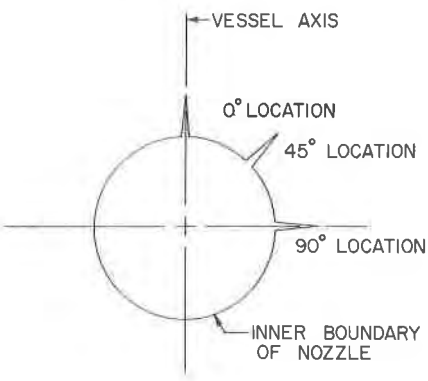


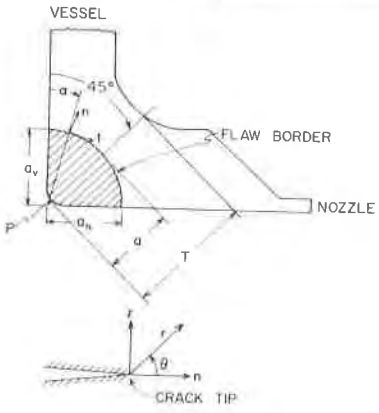


Figure 1 (a) Nozzle Model Dimensions (b) Photo of Model
(c) Crack Orientations (d) Problem Geometry and Notation

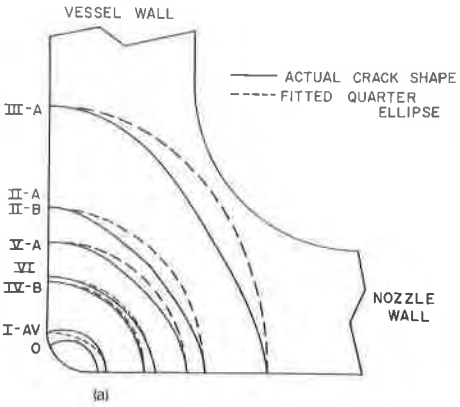


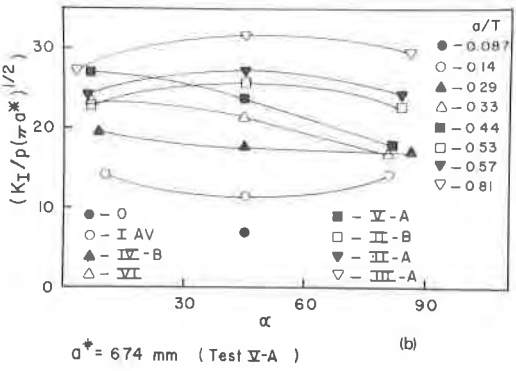


Figure 2 (a) Flaw Shapes and (b) SIF Distributions 0° Orientation

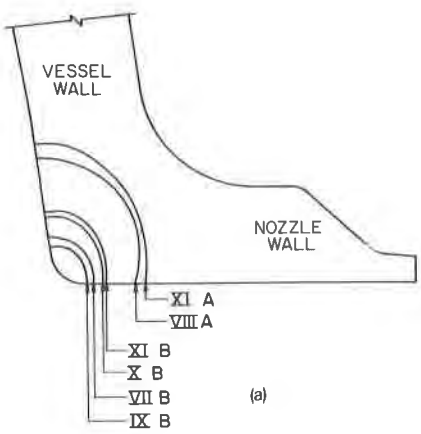


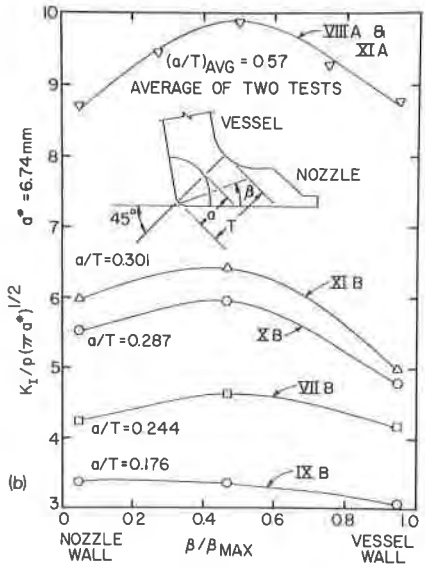


Figure 3 (a) Flaw Shapes and SIF Distributions 90° Orientation

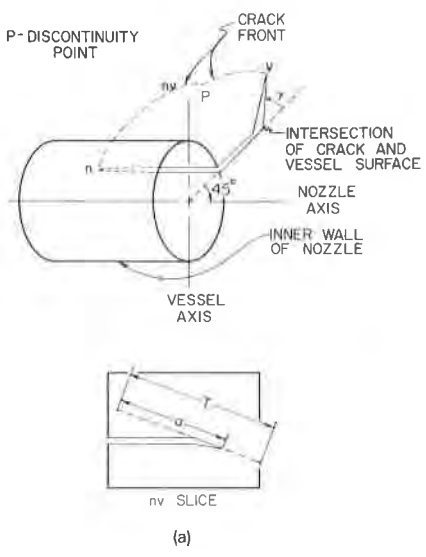


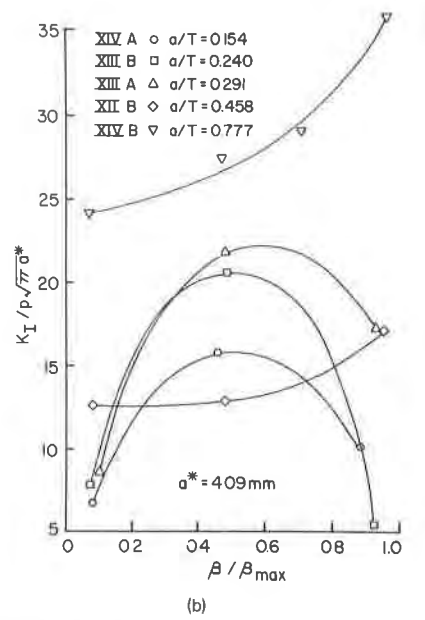


Figure 4 (a) Flaw Shapes and (b) SIF Distributions 45° Orientations

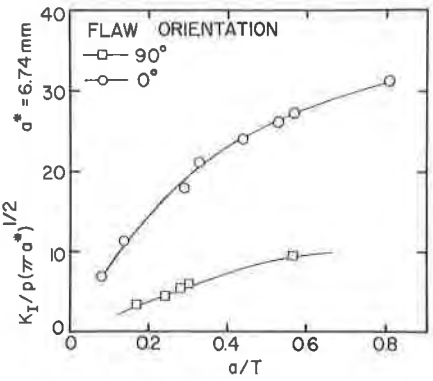


Figure 5 Comparison of 0° and 90° Flaw Orientation Results

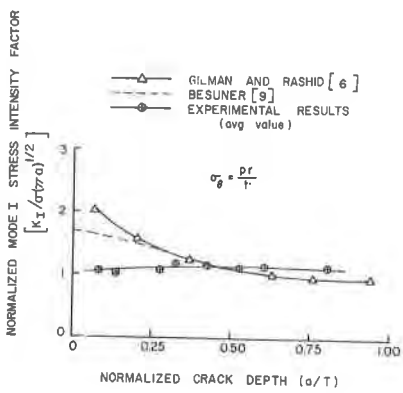


Figure 6 Comparison of Experimental Results with Analysis 0° Orientation

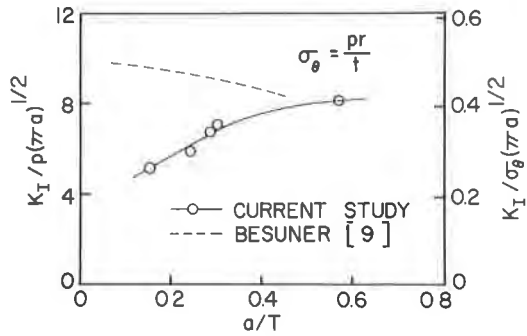


Figure 7 Comparison of Experimental Results with Analysis 90° Orientation

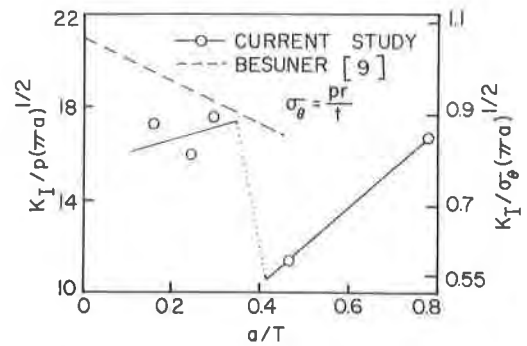


Figure 8 Comparison of Experimental Results with Analysis 45° Orientation